Anti-cancer activity of targeted pro-apoptotic peptides

H. Michael Ellerby, Wadih Arap, Lisa M. Ellerby, Renate Kain, Rebecca Andrusiak, Gabriel Del Rio, Stanislaw Krajewski, Christian R. Lombardo, Rammohan Rao, Erkki Ruoslahti, Dale E. Bredesen & Renata Pasqualini

Program on Aging and Cancer and Program on Cell Adhesion, The Burnham Institute, 10901 North Torrey Pines Rd., La Jolla, California 92037, USA
H.M.E., L.M.E., G.D.R., R.R. & D.E.B. present address: The Buck Center for Research in Aging, 8001 Redwood Blvd, Novato, California 94945, USA
R.K. present address: Clinical Institute for Clinical Pathology, Dept. Ultrastructural Pathology and Cell Biology, University of Vienna/AKH Wien, Währinger Gürtel 18-20, A-1090 Wien, Austria
W.A. & R.P. present address: The University of Texas M.D. Anderson Cancer Center, 1515 Holcombe Boulevard, Houston, Texas 77030, USA
Correspondence should be addressed to E.R., D.B. or R.P.; emails: ruoslahti, dbredesen or pasqualini@burnham-inst.org

We have designed short peptides composed of two functional domains, one a tumor blood vessel 'homing' motif and the other a programmed cell death-inducing sequence, and synthesized them by simple peptide chemistry. The 'homing' domain was designed to guide the peptide to targeted cells and allow its internalization. The pro-apoptotic domain was designed to be non-toxic outside cells, but toxic when internalized into targeted cells by the disruption of mitochondrial membranes. Although our prototypes contain only 21 and 26 residues, they were selectively toxic to angiogenic endothelial cells and showed anti-cancer activity in mice. This approach may yield new therapeutic agents.

Tumor cell survival, growth and metastasis require persistent new blood vessel growth[1–3] (angiogenesis). Consequently, a strategy has emerged to treat cancer by inhibiting angiogenesis[4]. Peptides have been described that selectively target angiogenic endothelial cells[5–8]. Conjugates made from these peptides and the anti-cancer drug doxorubicin induce tumor regression in mice with a better efficacy and a lower toxicity than doxorubicin alone[8]. There is also a functional class of cell death-inducing receptors, or 'dependence receptors', which have embedded pro-apoptotic amino-acid sequences[9,10]. These peptide domains are required for apoptosis induction by these receptors. The peptide fragments are thought to be released into the cytosol as cleavage products of caspase proteolysis, where they induce or potentiate apoptosis through unknown mechanisms[9,10]. However, such peptides, and structurally similar pro-apoptotic antibiotic peptides, although they remain relatively non-toxic outside of eukaryotic cells, induce mitochondrial swelling and mitochondria dependent cell-free apoptosis[10,11].

There are more than 100 naturally occurring antibiotic peptides, and their *de novo* design has received much attention[12–14]. Many of these peptides are linear, cationic and α-helix-forming. Some are also amphipathic, with hydrophobic residues distributed on one side of the helical axis and cationic residues on the other[15]. Because their cationic amino acids are attracted to the head groups of anionic phospholipids, these peptides preferentially disrupt negatively charged membranes. Once electrostatically bound, their amphipathic helices distort the lipid matrix (with or without pore formation), resulting in the loss of membrane barrier function[15,16]. Both prokaryotic cytoplasmic membranes and eukaryotic mitochondrial membranes (both the inner and the outer) maintain large transmembrane potentials, and have a high content of anionic phospholipids, reflecting the common ancestry of bacteria and mitochondria[15–19]. In contrast, eukaryotic plasma membranes (outer leaflet) generally have low membrane potentials, and are almost exclusively composed of zwitterionic phospholipids[16,18,20]. Many antibacterial peptides, therefore, preferentially disrupt prokaryotic membranes and eukaryotic mitochondrial membranes rather than eukaryotic plasma membranes.

If such nontoxic peptides were coupled to tumor targeting peptides that allow receptor-mediated internalization, the chimeric peptide would have the means to enter the cytosol of targeted cells, where it would be toxic by inducing mitochondrial-dependent apoptosis[10,11]. Thus, we designed targeted pro-apoptotic peptides composed of two functional domains. The targeting domain was designed to guide the 'homing' pro-apoptotic peptides to targeted cells and allow their internalization[8,21,22]. The pro-apoptotic domain was designed to be non-toxic outside of cells, but toxic when internalized into targeted cells by the disruption of mitochondrial membranes.

Design of the pro-apoptotic peptide

A computer-generated model and the sequence of one of our prototypes are shown in Fig. 1. For the targeting domain, we used either the cyclic (disulfide bond between cysteines) CNGRC peptide (Fig. 1) or the double-cyclic ACDCRGDCFC peptide (called RGD-4C), both of which have 'tumor-homing' properties[5,8] and for which there is evidence of internalization[8,21,22]. We synthesized this domain from all-L amino acids because of the presumed chiral nature of the receptor interaction. For the pro-apoptotic domain, we selected the synthetic 14-amino-acid peptide KLAKLAKKLAKLAK (Fig. 1), called $(KLAKLAK)_2$, because it killed bacteria at concentrations 1% of those required to kill eukaryotic cells[13]. We used the all-D enan-

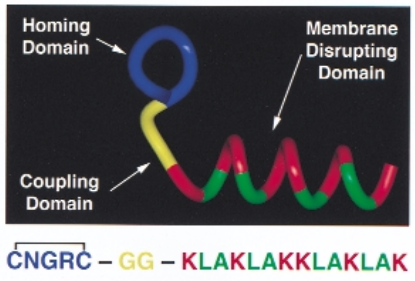

Fig. 1 Computer-generated model and amino-acid sequence of CNGRC-GG$_D$(KLAKLAK)$_2$. This peptide is composed of a 'homing' domain (blue) and a membrane-disrupting (pro-apoptotic) domain (red hydrophilic and green hydrophobic residues), joined by a coupling domain (yellow).

tiomer $_D$(KLAKLAK)$_2$ to avoid degradation by proteases[12,23]. This strategy was possible because such peptides disrupt membranes by chiral-independent mechanisms[23,24]. We coupled the targeting (CNGRC or RGD-4C) and pro-apoptotic $_D$(KLAKLAK)$_2$ domains with a glycinylglycine bridge (Fig. 1) to impart peptide flexibility and minimize potential steric interactions that would prevent binding and/or membrane disruption.

D(KLAKLAK)2 disrupts mitochondrial membranes

We evaluated the ability of $_D$(KLAKLAK)$_2$ to disrupt mitochondrial membranes preferentially rather than eukaryotic plasma membranes by mitochondrial swelling assays, in a mitochondria-dependent cell-free system of apoptosis, and by cytotoxicity assays[10]. There was morphological evidence of damage to mitochondrial membranes by electron microscopy. The peptide $_D$(KLAKLAK)$_2$ induced considerable mitochondrial swelling at a concentration of 10 μM (Fig. 2*a*). Mild swelling was evident even at 3 μM (data not shown), 1% the concentration required to kill eukaryotic cells (approximately 300 μM), as determined by the lethal concentration required to kill 50% of a cell monolayer (LC_{50}; Table 1). These results demonstrate that $_D$(KLAKLAK)$_2$ preferentially disrupts mitochondrial membranes rather than eukaryotic plasma membranes. Moreover, the peptide activated mitochondria-dependent cell-free apoptosis in a system composed of mitochondria suspended in cytosolic extract[10], as measured by characteristic caspase-3-processing from an inactive zymogen to active protease[25] (Fig. 2*b*). A non-α-helix-forming peptide, DLSLARLATARLAI (negative control), did not induce mitochondrial swelling (Fig. 2*a*), was inactive in the cell-free system (Fig. 2*b*) and was not lethal to eukaryotic cells[10]. We also analyzed morphologic alterations in isolated mitochondria by electron microscopy. The peptide $_D$(KLAKLAK)$_2$ induced abnormal mitochondrial morphology, whereas the control peptide DLSLARLATARLAI did not (Fig. 2*c*).

Targeted pro-apoptotic peptides induce apoptosis

We evaluated the efficacy and specificity of CNGRC-GG-$_D$(KLAKLAK)$_2$ in KS1767 cells, derived from Kaposi sarcoma[26,27] (Fig. 3*a–d*), and MDA-MB-435 human breast carcinoma cells[5,8] (Table 1). We used KS1767 cells because they bind the CNGRC targeting peptide just as endothelial cells do. This may relate to the endothelial origin of the KS1767 cells[27]. We used MDA-MB-435 cells as negative control cells because they do not bind the CNGRC targeting peptide[8]. Although CNGRC-GG-$_D$(KLAKLAK)$_2$ was considerably toxic to KS1617 cells, an equimolar mixture of uncoupled CNGRC and $_D$(KLAKLAK)$_2$ (negative control), or $_D$(KLAKLAK)$_2$ alone, was much less toxic, indicative of a targeting effect (Table 1). In contrast, CNGRC-GG-$_D$(KLAKLAK)$_2$ was not very toxic to MDA-MB-435 cells, which do not bind the CNGRC peptide (Table 1). The other targeted peptide (RGD-4C)-GG-$_D$(KLAKLAK)$_2$, showed toxic effects similar to those of CNGRC-GG-$_D$(KLAKLAK)$_2$ on KS1617 cells, whereas an equimolar mixture of uncoupled RGD-4C and $_D$(KLAKLAK)$_2$, used as a negative control, was not very toxic (Table 1; Fig. 3*c–d*).

Although evidence for internalization of CNGRC and RGD-4C into the cytosol of cells has been published[5,8,21,22], we directly demonstrated internalization using biotin-labeled peptides. CNGRC–biotin, but not untargeted CARAC–biotin, was internalized into the cytosol of cells (Fig. 3*e–f*). We also obtained direct evidence for internalization from experiments based on cell fractionation and mass spectrometry. CNGRC-GG-$_D$(KLAKLAK)$_2$, but not CARAC-GG-$_D$(KLAKLAK)$_2$, was indeed internalized and could be detected in mitochondrial as well as cytosolic fractions (data not shown).

Next, we evaluated the efficacy and specificity of CNGRC-GG-$_D$(KLAKLAK)$_2$ in a tissue culture model of angiogenesis[28]. During angiogenesis, capillary endothelial cells proliferate and migrate[1,2]. Cord formation is a type of migration that can be studied *in vitro* by a change in endothelial cell morphology from the usual 'cobblestones' to chains or cords of cells[27]. We tested the effect of CNGRC-GG-$_D$(KLAKLAK)$_2$ on normal human dermal microvessel endothelial cells (DMECs) in the angiogenic conditions of proliferation and cord formation and in the angiostatic condition of a monolayer maintained at 100% confluency.

The treatment of DMECs with 60 μM CNGRC-GG-$_D$(KLAKLAK)$_2$ led to a decrease in the percent viability over time compared with that of untreated controls, in the conditions of proliferation (Fig. 4*a*) or cord formation (Fig. 4*b*). In contrast, treatment with the untargeted peptide $_D$(KLAKLAK)$_2$ as a negative control led to a negligible loss in viability. Furthermore, the LC_{50} for proliferating or migrating DMECs treated with CNGRC-GG-$_D$(KLAKLAK)$_2$ was 10% of the LC_{50} for angiostatic DMECs maintained in a monolayer at 100% confluency (Table 1). This result indicates that CNGRC-GG-$_D$(KLAKLAK)$_2$ kills cells in angiogenic but not angiostatic conditions. The LC_{50} for the untargeted control $_D$(KLAKLAK)$_2$ in angiogenic con-

Table 1 LC_{50} (μM) for eukaryotic cells treated with targeted pro-apoptotic peptides

	DMEC			KS1767	MDA-MB-435
	Angiostatic	Angiogenic			
		Proliferation	Cord Form	Proliferation	Proliferation
$_d$(KLAKLAK)$_2$	492	346	368	387	333
CNGRC-GG-$_D$(KLAKLAK)$_2$	481	51[a]	34[a]	42[a]	415
(RGD-4C)-GG-$_D$(KLAKLAK)$_2$	–	–	–	10[a]	–

Results are means of three independent experiments. [a]P<0.03, t-test.

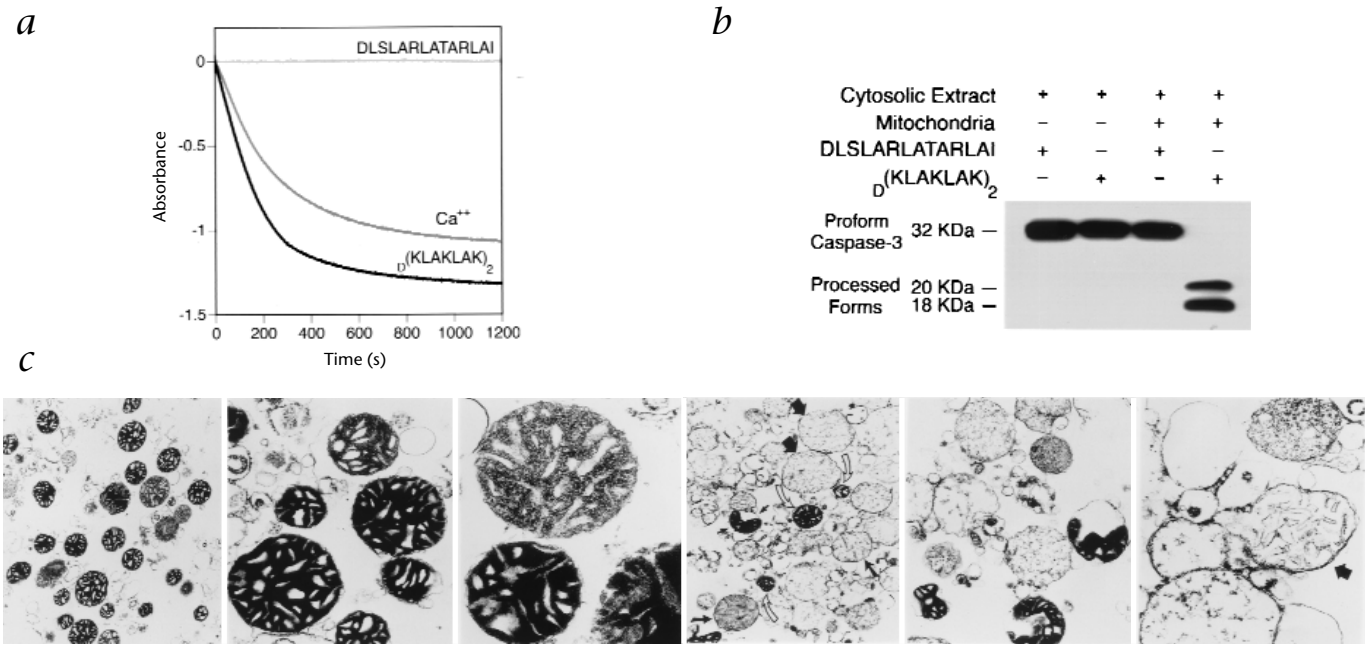

Fig. 2 $_D$(KLAKLAK)$_2$ disrupts mitochondrial membranes. ***a***, $_D$(KLAKLAK)$_2$ or Ca^{2+} (positive control) induced mitochondrial swelling, whereas the non-α-helix-former DLSLARLATARLAI (negative control) did not, as shown by mitochondrial swelling curves (optical absorbance spectrum). ***b***, $_D$(KLAKLAK)$_2$ activates cell-free apoptosis in a system composed of normal mitochondria and cytosolic extract, but DLSLARLATARLAI does not. An immunoblot of caspase-3 cleavage from proform (32-kDa) to processed forms (18- and 20-kDa) demonstrates a mitochondria-dependent cell-free apoptosis (left margin, sizes). Results were reproduced in two independent experiments. ***c***, Morphologic alterations in isolated mitochondria analyzed by electron microscopy. Mitochondria incubated for 15 min with 3 μM DLSLARLATARLAI show normal morphology (left panels). In contrast, mitochondria incubated for 15 min with 3 μM $_D$(KLAKLAK)$_2$ show extensive morphological changes. The damage to mitochondria progressed from the stage of focal matrix resolution (short black arrow), through homogenization and dilution of condensed matrix content with sporadic remnants of cristae (long black arrows), to extremely swollen vesicle-like structures (thick black arrows; bottom right, higher magnification); few mitochondria had normal morphology (open arrows). Ultrathin sections are shown. Original magnification, ×4,000–×40,000.

ditions was similar to the LC_{50} for CNGRC-GG-$_D$(KLAKLAK)$_2$ under angiostatic conditions. An equimolar mixture of uncoupled $_D$(KLAKLAK)$_2$ and CNGRC, a non-targeted form CARAC-GG-$_D$(KLAKLAK)$_2$, and a 'scrambled' form, CGRNC-GG-$_D$(KLAKLAK)$_2$, all gave results similar to those of $_D$(KLAKLAK)$_2$.

We also studied the mitochondrial morphology of DMECs in the condition of proliferation, after treatment with 60 μM CGRNC-GG-$_D$(KLAKLAK)$_2$ or untargeted $_D$(KLAKLAK)$_2$. The mitochondria in intact DMECs treated for 24 hours with the equimolar mixture CNGRC and $_D$(KLAKLAK)$_2$ remained morphologically normal (Fig. 4*d*), whereas those treated with CGRNC-GG-$_D$(KLAKLAK)$_2$ showed altered mitochondrial morphology, evident in approximately 80% of cells (Fig. 4*e*), before the cells rounded-up. Ultimately, the DMECs treated with CNGRC-GG-$_D$(KLAKLAK)$_2$ showed the classic morphological indicators of apoptosis, including nuclear condensation and fragmentation, as seen at 72 hours (Fig. 4 *f* and *g*)(ref. 10). Apoptotic cell death (Fig. 4*g*) was confirmed with an assay for

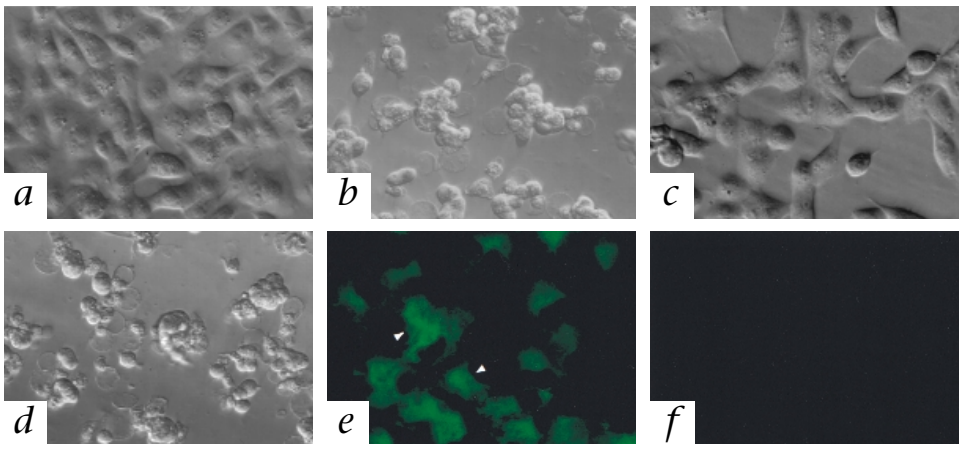

Fig. 3 CNGRC-GG-$_D$(KLAKLAK)$_2$ and (RGD-4C)-GG-$_D$(KLAKLAK)$_2$ induce apoptosis. ***a***, KS1767 cells treated with 100 μM of non-targeted CARAC-GG-$_D$(KLAKLAK)$_2$ (negative control) remain unaffected after 48 h. ***b***, KS1767 cells treated with 100 μM of CNGRC-GG-$_D$(KLAKLAK)$_2$ undergo apoptosis, as shown at 48 h. Condensed nuclei and plasma membrane blebbing are evident. ***c***, KS1767 cells treated with 10 μM of an equimolar mixture of (RGD-4C) and $_D$(KLAKLAK)$_2$ (negative control) remain unaffected after 48 h. ***d***, KS1767 cells treated with 10 μM of (RGD-4C)-GG-$_D$(KLAKLAK)$_2$ undergo apoptosis, as shown at 48 h. Condensed nuclei and plasma membrane blebbing are evident. Scale bar represents 250 μm. ***e*** and ***f***, KS1767 cells treated with 100 μM of CNGRC-biotin (*e*) or CARAC-biotin (*f*) for 24 h and subsequently treated with streptavidin FITC demonstrate internalization of CNGRC-biotin, but not CARAC-biotin, into the cytosol.

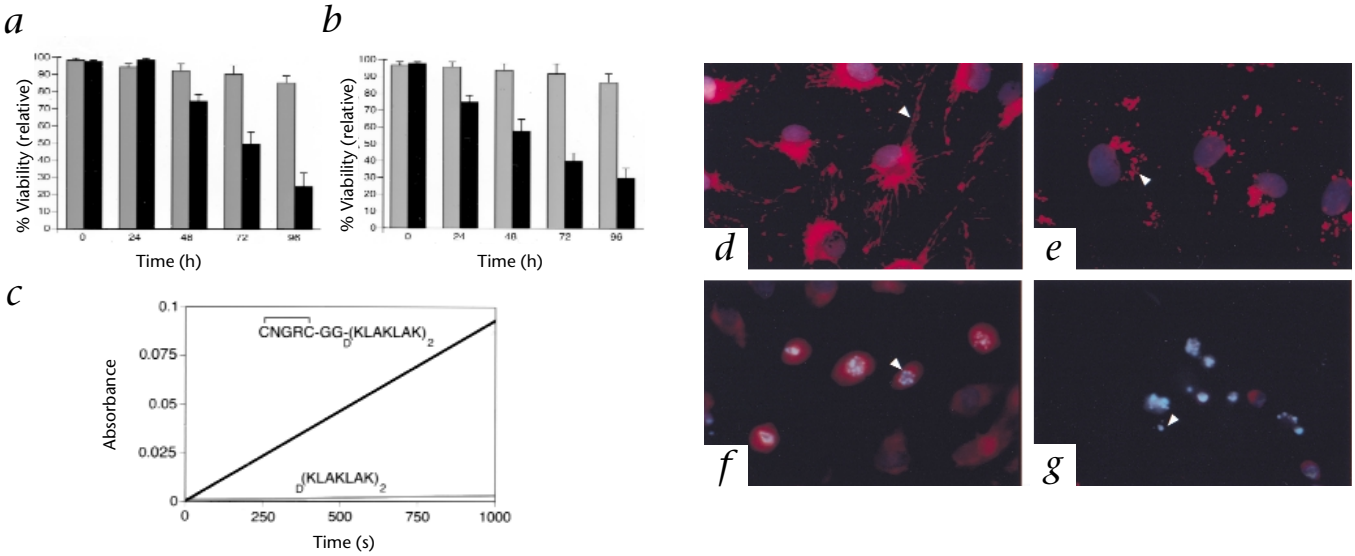

Fig. 4 CNGRC-GG-$_D$(KLAKLAK)$_2$ induces apoptosis and mitochondrial swelling in DMECs. ***a***, Proliferating DMECs treated with CNGRC-GG-$_D$(KLAKLAK)$_2$ (filled bars) lose viability (apoptosis) over time ($P < 0.02$), but those treated with the control peptide $_D$(KLAKLAK)$_2$ (gray bars) do not ($P < 0.05$). ***b***, Cord-forming DMECs lose viability (apoptosis) over time (filled bars), but those treated with $_D$(KLAKLAK)$_2$ (gray bars) do not ($P < 0.05$). ***c***, Apoptotic cell death was confirmed with an assay for caspase 3 activity, as shown by the hydrolysis of DEVD-pNA with time. Results were reproduced in three independent experiments. ***d***, Proliferating DMECs show normal nuclear (blue) and mitochondrial (red) morphology after 24 h of treatment with a mixture of 100 μM $_D$(KLAKLAK)$_2$ and CNGRC. ***e–g***, Proliferating DMECs treated with 100 μM CNGRC-GG-$_D$(KLAKLAK)$_2$. After 24 h (*e*), cells show normal nuclear (blue) but abnormal mitochondrial (red) morphology. Mitochondrial swelling and dysfunction is shown by a decrease in fluorescence intensity and a change in morphology from an extended lace-like network to a condensed clumping of spherical structures. Classic morphological indicators of mid- to late apoptosis (for example, condensed and fragmented nuclei) are evident at 48 h (*f*) and 72 h (*g*) (arrow).

caspase 3 activity[10]. We also tested a caspase inhibitor for its effect on cell death induced by CNGRC-GG-$_D$(KLAKLAK)$_2$. We used Kaposi sarcoma cells, as these cells bind CNGRC. The inhibitor zVAD.fmk, at a concentration (25 μM) that inhibits caspases but not non-caspase proteases, inhibited the cell death induced by CNGRC-GG-$_D$(KLAKLAK)$_2$ (data not shown). This result is compatible with the earlier demonstration that the CNGRC-GG-$_D$(KLAKLAK)$_2$ peptide is pro-apoptotic. Although the relatively early mitochondrial swelling is consistent with the putative mechanism of action, that is, a direct activation of the apoptotic machinery, we cannot rule out the possibility that the peptides actually kill by inducing some irreversible damage to cells which then activates the apoptotic program.

In addition to the fluorescence studies shown above, we studied cultured cells by electron microscopy to confirm that CNGRC-GG-$_D$(KLAKLAK)$_2$ induces abnormal mitochondrial morphology in intact cells (Fig. 5). Kaposi sarcoma-derived KS1767 cells treated with the control peptide CARAC-GG-$_D$(KLAKLAK)$_2$ for 72 hours showed no overall changes, with no or very minor changes in the mitochondria (Figs. 5*a–c*). In contrast, the mitochondria in KS1767 cells incubated for 12 hours

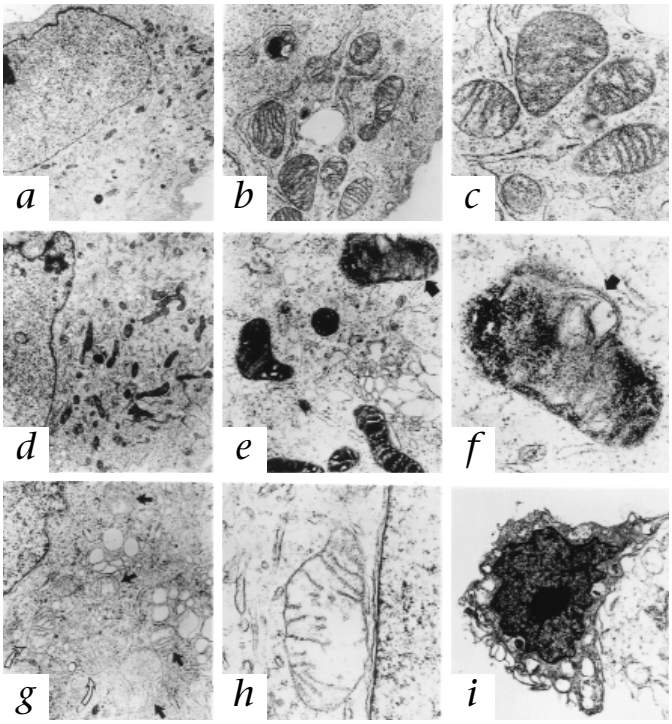

Fig. 5 Electron microscopic studies of cultured cells. *a–c*, KS1767 cells treated with 100 μM CARAC-GG-$_D$(KLAKLAK)$_2$ for 72 h show the representative ultrastructural details of normal cells, with no or negligible changes seen in the mitochondria. Original magnifications: ***a***, ×4,000; ***b***, ×25,000; ***c***, ×45,000. ***d–f,*** In contrast, the mitochondria in KS1767 cells incubated for 12 h with 100 μM CNGRC-GG-$_D$(KLAKLAK)$_2$ begin to show a condensed appearance and vacuolization despite a relatively normal cell morphology (black arrows). Original magnifications: *d*, ×12,000; *e*, ×20,000; *f*, ×45,000). *g* and *h*, Progressive damage to KS1767 cells is evident after 24 h, when many mitochondria show typical large matrix compartments and prominent cristae, ultrastructural features of low level of oxidative phosphorylation. Original magnifications: ***g***, ×12,000; ***h***, ×40,000. Some of the swollen mitochondria (*g*, black arrows) are similar in appearance to those in isolated mitochondria treated with 100 μM $_D$(KLAKLAK)$_2$ (Fig. 2*c*, bottom right). ***i***, In some cells, this process progressed to a final stage, with extensive vacuolization and the pyknotic, condensed nuclei typical of apoptosis. Original magnification, ×8,000.

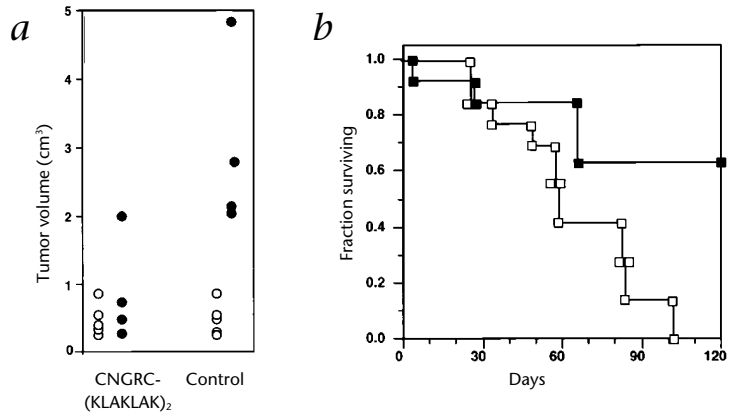

Fig. 6 Treatment of nude mice bearing MDA-MB-435-derived human breast carcinoma xenografts with CNGRC-GG-$_D$(KLAKLAK)$_2$. ***a***, Tumors treated with CNGRC-GG-$_D$(KLAKLAK)$_2$ are smaller than control tumors treated with CARAC-GG-$_D$(KLAKLAK)$_2$, as shown by differences in tumor volumes between day 1 (○) and day 50 (●). P = 0.027, t-test. One mouse in the control group died before the end of the experiment. ***b***, Mice treated with CNGRC-GG-$_D$(KLAKLAK)$_2$ (■) survived longer than control mice treated with an equimolar mixture of $_D$(KLAKLAK)$_2$ and CNGRC (□), as shown by a Kaplan-Meier survival plot (n = 13 animals/group). $P < 0.05$, log-rank test.

with CNGRC-GG-$_D$(KLAKLAK)$_2$ showed abnormal condensation and vacuolization despite a relatively preserved cell morphology (Fig. 5*d–f*, black arrows). Progressive cellular damage could be seen after 24 hours, when many mitochondria showed ultrastructural features of low-level oxidative phosphorylation (Fig. 5*g* and *h*); in later stages, some of the damaged mitochondria (Fig. 5g, black arrows) showed profound changes, as seen in the isolated mitochondria treated with $_D$(KLAKLAK)$_2$ (Fig. 2*c*, right lower panel). In some cells, this process progressed to a late apoptotic stage. Typical vacuolization and condensed nuclei became evident (Fig. 5*i*). These results show that the mitochondria underwent changes in morphology and function that were well-represented by a progression from a state of normal morphology and normal oxidative phosphorylation (Fig. 5*a*) to a state of condensed morphology and a high rate of oxidative phosphorylation (Fig. 5*d*) to a final edemic state (Fig. 5*g*) associated with a low energy level.

Treatment of nude mice bearing human tumor xenografts with CNGRC-GG-$_D$(KLAKLAK)$_2$ and (RGD-4C)-GG-$_D$(KLAKLAK)$_2$

Given our results in culture, we proceeded to test both targeted pro-apoptotic peptides *in vivo*, using nude mice with human MDA-MD-435 breast carcinoma xenografts. Tumor volume in the groups treated with CNGRC-GG-$_D$(KLAKLAK)$_2$ was on average 10% that of control groups (Fig. 6*a*); survival was also longer in these groups than in control groups (Fig. 6*b*). The control was a non-targeted 'mimic' CARAC-GG-$_D$(KLAKLAK)$_2$ peptide; the CARAC sequence has a charge, size and general structure similar to that of CNGRC. Some of the mice treated with CNGRC-GG-$_D$(KLAKLAK)$_2$ outlived control mice by several months, indicating that both primary tumor growth and metastasis were inhibited by CNGRC-GG-$_D$(KLAKLAK)$_2$. Treatment in nude mice bearing MDA-MD-435 breast carcinoma xenografts with (RGD-4C)-GG-$_D$(KLAKLAK)$_2$ also resulted in a significantly reduced tumor and metastatic burden (Fig. 7). Experimental parameters included tumor volumes before and after treatment (Fig. 7*a*), wet weights of the tumors (Fig. 7*b*, right) and weight of lung metastases (Fig. 7*b*, left). The control group was treated with an equimolar mixture of RGD-4C and $_D$(KLAKLAK)$_2$. Histopathological and TUNEL analysis showed cell death in the treated tumors and evidence of apoptosis and necrosis (data not shown).

To assess toxicity in mice without tumors, we have administered CNGRC-GG-$_D$(KLAKLAK)$_2$ or (RGD-4C)-GG-$_D$(KLAKLAK)$_2$ to both immunocompetent (balb/c) and to immunodeficient (balb/c nude) mice at a dose of 250 µg/mouse per week for eight doses. No apparent toxicities have been found in 3 months. Moreover, in these conditions, the peptides are not immunogenic, as determined by ELISA of blood obtained from the immunocompetent mice (data not shown).

We have also evaluated the stability of the CNGRC-GG-$_D$(KLAKLAK)$_2$ and (RGD-4C)-GG-$_D$(KLAKLAK)$_2$ peptides *ex vivo* and in mice. We analyzed the two targeted peptides using mass spectrometry. In the first set of experiments, the targeted peptides were pre-mixed with whole blood and incubated at 37 °C.

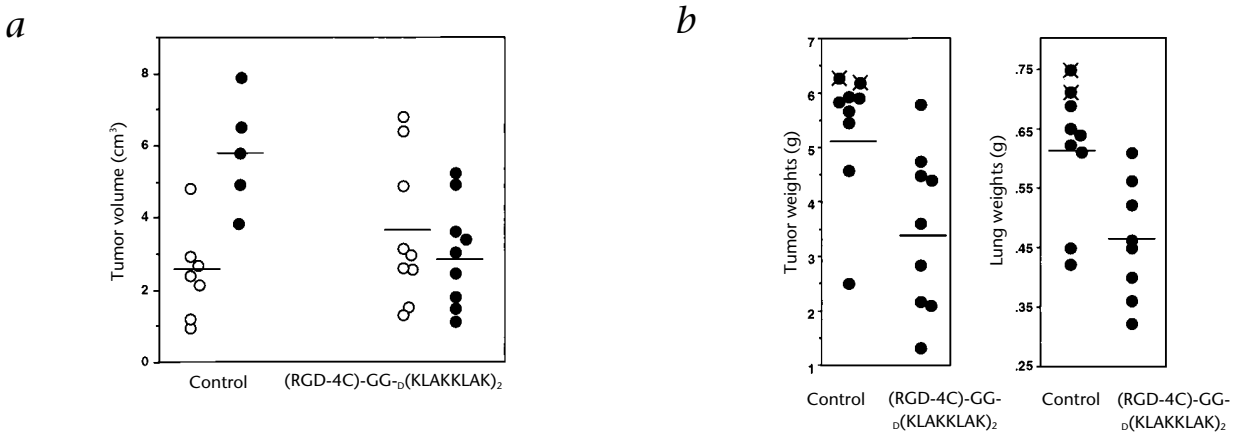

Fig. 7 Treatment of nude mice bearing MDA-MB-435-derived human breast carcinoma xenografts with (RGD-4C)-GG-$_D$(KLAKLAK)$_2$. ***a***, Tumors treated with (RGD-4C)-GG-$_D$(KLAKLAK)$_2$ are smaller than control tumors treated with an equimolar mixture of RGD-4C peptide and $_D$(KLAKLAK)$_2$. Tumor volumes were assessed on day 1 (○) and day 90 (●). P = 0.027, t-test. ***b***, Tumor weights (right) and lung metastatic burden (left) are also decreased in mice treated with (RGD-4C)-GG-$_D$(KLAKLAK)$_2$; these were measured when the experiment ended, on day 110 (n = 9 animals/group). $P < 0.05$, t-test.

The peptides were intact up to 1 hour in these conditions. In the second set of experiments, mice were injected intravenously with the two targeted peptides and blood samples were analyzed; the peptides were present at 10 minutes after administration (data not shown). We chose these short circulation times to coincide with the experimental conditions established for 'homing' of targeted peptides *in vivo*[5,7,8].

Targeted pro-apoptotic peptides represent a potential new class of anti-cancer agents; their activity may be optimized for maximum therapeutic effect by adjusting properties such as residue placement, domain length, peptide hydrophobicity and hydrophobic moment[29]. Beyond this, future targeted pro-apoptotic peptides might be designed to disrupt membranes using a completely different type of pro-apoptotic domain such as β-strand/sheet-forming peptides[30]. Our results provide a glimpse at a new cancer therapy combining two levels of specificity: 'homing' to targeted cells and selective apoptosis of such cells after entry.

Methods

Reagents. Human recombinant vascular endothelial growth factor (VEGF; PharMingen, San Diego, California), antibody against caspase-3 (Santa Cruz Biotechnology, Santa Cruz, California), streptavidin FITC (Sigma) and N-acetyl-Asp-Glu-Val-Asp-pNA (DEVD-pNA; BioMol, Plymouth Meeting, Pennsylvania) were obtained commercially. Peptides were synthesized to our specifications at greater than 90% purity by HPLC (DLSLARLATARLAI, Coast (San Diego, California); all other peptides, AnaSpec (San Jose, California).

The computer-generated model was made with Insight II (Molecular Simulations, San Diego, California) running on an O_2 work station (Silicon Graphics, Mountain View, California)

Cell culture. Dermal microvessel endothelial cells (DMECs) were grown in CADMEC Growth Media™ (media and cells from Cell Applications, San Diego, California). DMECs were then cultured in three experimental conditions: proliferation (30% confluency in a growth media supplemented with 500 ng/ml VEGF); no proliferation (100% confluency in media formulated to maintain a monolayer); and cord formation (60% confluency (required for induction) in media formulated to induce cord formation). KS1767 and MDA-MB-435 cells were cultured as described[5,8,27,28].

Internalization assay. KS1767 cells grown on coverslips were treated with 100 μM biotin-labeled CNGRC or biotin-labeled CARAC (negative control) for 24 h. Streptavidin FITC was added to the coverslips, and cells were then viewed on an inverted microscope (Nikon TE 300) using a FITC filter.

Mitochondrial swelling assays. Rat liver mitochondria were prepared as described[10]. The concentrations used were 10 μM $_D$(KLAKLAK)$_2$, 10 μM DLSLARLATARLAI (negative control), or 200 μM Ca^{2+} (positive control). The peptides were added to mitochondria in a cuvette, and swelling was quantified by measuring the optical absorbance at 540 nm.

Cell-free apoptosis assays. Cell-free systems were reconstituted as described[10]. For the mitochondria-dependent reactions, rat liver mitochondria were suspended in normal (non-apoptotic) cytosolic extracts of DMECs. The peptides were added at a concentration of 100 μM. After incubation for 2 h at 30 °C or 37 °C, mitochondria were removed by centrifugation, and the supernatant was analyzed by SDS–PAGE and immunoblotting (12% gels, BioRad, Richmond, California). Proteins were transferred to PVDF membranes (BioRad, Richmond, California) and incubated with antibody against caspase-3, followed by ECL detection (Amersham).

Caspase activity of cell lysates. The caspase activity of DMEC lysates was measured as described[10]. Aliquots of cell lysates (1 μl lysate; 8–15 mg/ml) were added to 100 μM DEVD-pNA (100 μl; 100 mM HEPES, 10% sucrose, 0.1% CHAPS and 1 mM DTT, pH 7.0). Hydrolysis of DEVD-pNA was monitored by spectrophotometry (400 nm) at 25 °C.

Morphological quantification of cellular apoptosis. Percent viability and LC_{50} (Table 1) were determined by apoptotic morphology[10]. For the percent viability assay, DMECs were incubated with 60 μM active peptide or control peptide. Cell culture medium was aspirated at various times from adherent cells, and the cells were gently washed once with PBS at 37 °C. Then, a 20-fold dilution of the dye mixture (100 μg/ml acridine orange and 100 μg/ml ethidium bromide) in PBS was gently pipetted on the cells, which were viewed on an inverted microscope (Nikon TE 300). The cell death seen was apoptotic cell death and was confirmed by a caspase activation assay. Not all cells progressed through the stages of apoptosis at the same time. At the initial stages, a fraction of the cells were undergoing early apoptosis. At later stages, this initial fraction had progressed to late apoptosis and even to the necrotic-like stage associated with very late apoptosis (for example, loss of membrane integrity in apoptotic bodies). However, these cells were joined by a new fraction undergoing early apoptosis. Thus, cells with nuclei showing margination and condensation of the chromatin and/or nuclear fragmentation (early/mid-apoptosis; acridine orange-positive) or with compromised plasma membranes (late apoptosis; ethidium bromide-positive) were considered not viable. At least 500 cells per time point were assessed in each experiment. Percent viability was calculated relative to untreated controls. LC_{50} for monolayer, proliferation (60% confluency), and cord formation were assessed at 72 h.

Mitochondrial morphology. DMECs after 24 and 72 h of treatment with peptide were incubated for 30 min at 37 °C with a mitochondrial stain (100 nM MitoTracker Red™ CM-H_2XRos; the nonfluorescent, reduced form of the compound) and a nuclear stain (500 nm DAPI; Molecular Probes, Eugene, Oregon). Mitochondria were then visualized under fluorescence microscopy (100x objective) under an inverted microscope using a triple wavelength filter set (Nikon).

Electron microscopy. Rat liver mitochondria were prepared as described[10]. The mitochondria were incubated either with a control peptide (DLSLARLATARLAI) or with 3 μM $_D$(KLAKLAK)$_2$. The effects of the treatment were assessed at different times (Fig. 2*c*). Kaposi sarcoma cells were collected from 24-well Biocoat Cell culture inserts for electron microscopy (Becton Dickinson, Franklin Lakes, New Jersey). Cell monolayers at 80% confluency were exposed to either 100 μM CARAC-GG-$_D$(KLAKLAK)$_2$ (control) or CNGRC-GG-$_D$(KLAKLAK)$_2$ (targeted) (Fig. 5). All specimens were fixed with 3% glutaraldehyde in 0.1 M potassium phosphate buffer, pH 7.4 for 30 to 45 min at the room temperature, followed by postfixation with aqueous 1% osmium tetroxide and 2% uranyl acetate. After dehydration using a graded series of ethanol rinses, tissues were embedded in resin. Ultrathin sections after additional counterstainings were viewed and photographed on an electron microscope (Hitachi H-600).

Human tumor xenografts. MDA-MB-435-derived tumor xenografts were established in female nude mice 2 months old (Jackson Labs, Bar Harbor, Maine) as described[33]. The mice were anesthetized with Avertin as described[31]. The peptides were administered at a dose of 250 μg/week per mouse, given slowly through the tail vein in a volume of 200 μl. Three-dimensional measurements of tumors were made by caliper on anesthetized mice, and were used to calculate tumor volume[5,8]. Then, tumors and lungs were surgically removed and the wet weights recorded. Animal experimentation was reviewed and approved by the Institute's Animal Research Committee.

Acknowledgments

We thank W.K. Cavenee and G. Salvesen for comments and critical reading of the manuscript. This work was supported by grants CA74238, CA28896 (to ER) NS33376 and Cancer Center support grant CA30199 (to R.P., D.B. and E.R.) from the National Cancer Institute (USA), and DAMD17-98-1-8581 (to D.B. and R.P.) from the DOD-PCRP. H.M.E. is the recipient of a NS10050 NRSA senior fellowship grant. W.A. is the recipient of a CaP CURE award.

RECEIVED 11 MAY; ACCEPTED 30 JUNE 1999

1. Risau, W. Mechanisms of angiogenesis. *Nature* **386**, 671–674 (1997).
2. Zetter, B.R. Angiogenesis and tumor metastasis. *Annu. Rev. Med.* **49**, 407–424

(1998).
3. Bicknell, R. in *Tumour Angiogenesis.* (eds. Bicknell, R., Lewis, C.E. & Ferrara, N.) 19–28 (Oxford University Press, Oxford 1997).
4. Folkman, J. in *Cancer: Principles and Practice of Oncology*. (eds. DeVita, V.T., Hellman, S. & Rosenberg, S.A.) 3075–3087 (Lippincott-Raven, New York, 1997).
5. Pasqualini, R., Koivunen, E. & Ruoslahti, E. αv integrins as receptors for tumor targeting by circulating ligands. *Nature Biotechnol.* **15,** 542–546 (1997).
6. Arap, W., Pasqualini, R. & Ruoslahti, E. Chemotherapy targeted to tumor vasculature. *Curr. Opin. Oncol.* **10**, 560–565 (1998).
7. Pasqualini, R., Arap, W., Rajotte, D. & Ruoslahti, E. in *Phage Display of Proteins and Peptides* (eds. Barbas, C., Burton, D., Silverman, G. & Scott, J.) (Cold Spring Harbor, New York, in the press).
8. Arap, W., Pasqualini, R. & Ruoslahti, E. Cancer treatment by targeted drug delivery to tumor vasculature in a mouse model. *Science* **279,** 377–380 (1998).
9. Bredesen D.E. *et al.* P75(NTR) and the concept of cellular dependence – seeing how the other half die. *Cell Death Differ.* **5**, 365–371 (1998).
10. Ellerby, H.M. *et al.* Establishment of a cell-free system of neuronal apoptosis: comparison of premitochondrial, mitochondrial, and postmitochondrial phases. *J. Neurosci.* **17,** 6165–6178 (1997).
11. Mehlen, P. *et al.* The DCC gene product induces apoptosis by a mechanism requiring receptor proteolysis. *Nature* **395**, 801–804 (1998).
12. Bessalle, R., Kapitkovsky, A., Gorea, A., Shalit, I. & Fridkin, M. All-D-magainin: chirality, antimicrobial activity and proteolytic resistance. *FEBS Lett.* **274,** 151–155 (1990).
13. Javadpour, M.M. *et al. De novo* antimicrobial peptides with low mammalian cell toxicity. *J. Med. Chem.* **39,** 3107–3113 (1996).
14. Blondelle, S.E. & Houghten, R.A. Design of model amphipathic peptides having potent antimicrobial activities. *Biochemistry* **31,** 12688–12694 (1992).
15. Epand, R.M. in *The Amphipathic Helix* (CRC, Boca Raton, Florida, 1993).
16. de Kroon, A., Dolis, D., Mayer, A., Lill, R. & de Kruijff, B. Phospholipid composition of highly purified mitochondrial outer membranes of rat liver and Neurospora crassa. Is cardiolipin present in the mitochondrial outer membrane? *Biochim. Biophys. Acta* **1325**, 108–116 (1997).
17. Matsuzaki, K., Murase, O., Fujii, N. & Miyajima, K. Translocation of a channel-forming antimicrobial peptide, magainin 2, across lipid bilayers by forming a pore. *Biochemistry* **34**, 6521–6526 (1995).
18. Hovius, R., Thijssen, J., van der Linden, P., Nicolay, K. & de Kruijff, B. Phospholipid asymmetry of the outer membrane of rat liver mitochondria: Evidence for the presence of cardiolipin on the outside of the outer membrane. *FEBS Lett.* **330,** 71–76 (1993).
19. Baltcheffsky, H., & Baltcheffsky, M. in *Mitochondria and Microsomes* (eds. Lee, C.P., Schatz, G., Dallner, G.) 519–540 (Addison-Wesley, Reading, Massachusetts, 1981).
20. Daum, G. Lipids of Mitochondria. *Biochim. Biophys. Acta* **882,** 1–42 (1985).
21. Hart, S.L. *et al.* Cell binding and internalization by filamentous phage displaying a cyclic Arg-Gly-Asp-containing peptide. *J. Biol. Chem.* **269,** 12468–12474 (1994).
22. Bretscher, M.S. Endocytosis and recycling of the fibronectin receptor in CHO cells. *EMBO J.* **8,** 1341–1348 (1989).
23. Dathe, M. *et al.* Hydrophobicity, hydrophobic moment, and angle subtended by charged residues modulate antibacterial and haemolytic activity of amphipathic helical peptides. *FEBS Lett.* **403,** 208–212 (1997).
24. Alvarez-Bravo, J., Kurata, S. & Natori, S. Novel synthetic antimicrobial peptides effective against methicillin-resistant *Staphylococcus aureus. Biochem. J.* **302,** 535–538 (1994).
25. Alnemri, E.S. *et al.* ICE/CED-3 protease nomenclature. *Cell* **87**, 171 (1996).
26. Hernier, B.G. *et al.* Characterization of a human Kaposi's sarcoma cell line that induces angiogenic tumors in animals. *AIDS* **8**, 575–581 (1994).
27. Samaniego, F. *et al.* Vascular endothelial growth factor and basic fibroblast growth factor present in Kaposi's sarcoma (KS) are induced by inflammatory cytokines and synergize to promote vascular permeability and KS lesion development. *Amer. J. Path.* **152,** 1433–1443 (1998).
28. Goto, F., Goto, K., Weindel, K. & Folkman, J. Synergistic effects of vascular endothelial growth factor and basic fibroblast growth factor on the proliferation and cord formation of bovine capillary endothelial cells within collagen gels. *Lab. Invest.* **69**, 508–517 (1993).
29. Wade, D. *et al.* All-D amino acid-containing channel-forming antibiotic peptides. *Proc. Natl Acad. Sci. USA* **87**, 4761–4765 (1990).
30. Mancheno, J.M., Martinez del Pozo, A., Albar, J.P., Onaderra, M. & Gavilanes, J.G. A peptide of nine amino acid residues from α-sarcin cytotoxin is a membrane-perturbing structure. *J. Peptide Res.* **51**, 142–148 (1998).
31. Pasqualini, R. & Ruoslahti, E. Organ targeting *in vivo* using phage display peptide libraries. *Nature* **380,** 36–366 (1996).